

Dynamical Origin of Quantum Probabilities

Antony Valentini¹

*Perimeter Institute for Theoretical Physics,
35 King Street North, Waterloo, Ontario N2J 2W9, Canada.*²

*Augustus College,
14 Augustus Road, London SW19 6LN, England.*³

Hans Westman⁴

*Department of Astronomy and Astrophysics,
Chalmers University of Technology,
41296 Göteborg, Sweden.*

We study the origin of the Born probability rule $\rho = |\psi|^2$ in the de Broglie-Bohm pilot-wave formulation of quantum theory. It is argued that quantum probabilities arise dynamically, and have a status similar to thermal probabilities in ordinary statistical mechanics. This is illustrated by numerical simulations for a two-dimensional system. We show that a simple initial ensemble with a non-standard distribution $\rho \neq |\psi|^2$ of particle positions evolves towards the quantum distribution to high accuracy. The relaxation process $\rho \rightarrow |\psi|^2$ is quantified in terms of a coarse-grained H -function (equal to minus the relative entropy of ρ with respect to $|\psi|^2$), which is found to decrease approximately exponentially over time, with a time constant that accords with a simple theoretical estimate.

¹email: avalentini@perimeterinstitute.ca

²Corresponding address.

³Permanent address.

⁴email: hawe@fy.chalmers.se

1 Introduction

In the de Broglie-Bohm pilot-wave formulation of quantum theory [1–10], the quantum state of an individual system is supplemented by a deterministic trajectory in configuration space. It is usually assumed that an ensemble of systems with wave function $\psi(q, t)$ (in configuration space) has configurations q distributed according to the Born probability rule $\rho(q, t) = |\psi(q, t)|^2$. More precisely, it is assumed that $\rho(q, 0) = |\psi(q, 0)|^2$ at some initial time $t = 0$, the equations of motion then guaranteeing that this quantum distribution is preserved at all later times.

The status of this assumption, that $\rho = |\psi|^2$ at some initial time, has been the subject of debate. Soon after Bohm’s first papers on the theory appeared [2], Pauli objected that taking a particular distribution $\rho = |\psi|^2$ as an initial condition was unjustified in a fundamentally deterministic theory [11]. Similarly, it was pointed out by Keller [12] that $\rho = |\psi|^2$ should be derived from the dynamics, in order for quantum theory truly to emerge as the statistical mechanics of an underlying deterministic theory.

Despite these criticisms, Bohm had in fact already suggested in his original papers that the distribution $\rho = |\psi|^2$ had a status similar to that of thermal equilibrium in ordinary statistical mechanics, and he had conjectured that this distribution could be derived by appropriate statistical-mechanical arguments. In a subsequent paper, Bohm studied the specific case of an ensemble of two-level molecules subjected to random external collisions, and argued that an initial nonequilibrium distribution $\rho \neq |\psi|^2$ would relax to the equilibrium state $\rho = |\psi|^2$ [13]. A general argument for relaxation was not given, however. A year later, in response to the criticisms of Pauli and Keller, and motivated by the difficulties in formulating a relaxation argument for an arbitrary system, Bohm and Vigier modified the theory by introducing stochastic ‘fluid fluctuations’ that drive the required process $\rho \rightarrow |\psi|^2$ for a general system [14].

Most subsequent presentations of the original (deterministic) theory have taken $\rho = |\psi|^2$ as an axiom. Usually, it is simply assumed that any ensemble prepared at time $t = 0$ with wave function $\psi(q, 0)$ will have a distribution $\rho(q, 0) = |\psi(q, 0)|^2$ of actual configurations q . Alternatively, $|\psi|^2$ has been regarded as the natural measure of probability or ‘typicality’ for initial configurations of the whole universe (taking ψ to be the universal wave function), yielding the Born rule for all subsystems at all times [15].

However, a quite general argument for the relaxation $\rho \rightarrow |\psi|^2$ may be framed in terms of an analogue of the classical coarse-graining H -theorem, based on the H -function

$$H = \int dq \rho \ln(\rho/|\psi|^2) \tag{1}$$

(equal to minus the relative entropy of ρ with respect to $|\psi|^2$) [16, 4, 17]. Like its classical counterpart, this theorem provides a general mechanism in terms of which one can understand how equilibrium is approached, while not proving that equilibrium is actually reached (see Sect. 5 below).

A relaxation timescale τ – analogous to the scattering time of classical kinetic theory – may be defined in terms of time derivatives of the coarse-grained H -function. For a particle of mass m , whose wave function has a quantum energy spread ΔE , the timescale is estimated to be [17]

$$\tau \sim \frac{1}{\varepsilon} \frac{\hbar^2}{m^{1/2}(\Delta E)^{3/2}} \quad (2)$$

where ε is the coarse-graining length. One expects τ to be the timescale over which there will be a significant approach to equilibrium. This rough estimate agrees quite closely with numerical simulations for particles moving in one spatial dimension [17].

In this paper, we study the relaxation $\rho \rightarrow |\psi|^2$ numerically, for the more realistic case of particles moving in two spatial dimensions. We shall see that if ψ is a superposition of energy eigenstates, the de Broglie-Bohm velocity field varies extremely rapidly in general, particularly in regions where $|\psi|$ is small. The resulting particle trajectories have a very complicated structure. Starting from a simple nonequilibrium distribution $\rho_0 \neq |\psi_0|^2$ at $t = 0$, the relaxation $\rho \rightarrow |\psi|^2$ takes place rather efficiently, on a timescale of order (2). And a plot of the coarse-grained H -function against time shows an approximately exponential decay, with time constant of order (2).

We interpret these results as further evidence that, in the pilot-wave formulation of quantum theory, the Born distribution $\rho = |\psi|^2$ should not be regarded as an axiom. Rather, it should indeed be seen as dynamically generated, in the same sense that one usually regards thermal equilibrium as arising from a process of relaxation based on some underlying dynamics.

In Sect. 2, we introduce pilot-wave dynamics for a single particle in a two-dimensional box. In Sect. 3, we illustrate the character of the trajectories. In Sect. 4, we introduce a nonequilibrium ensemble of systems, and show in detail how the ensemble evolves towards $\rho = |\psi|^2$. In Sect. 5 we show how the relaxation may be quantified in terms of the coarse-grained H -function, which is found to decay approximately exponentially with time, on a timescale of order (2). In Sect. 6, we discuss the significance of these results, addressing some relevant issues in the foundations of statistical mechanics.

2 Pilot-Wave Dynamics in Two Dimensions

Consider a single particle of unit mass, moving in a potential V in two spatial dimensions. The system has a configuration $q = (x, y)$, and wave function $\psi = \psi(x, y, t)$ (assuming a pure state) satisfying the Schrödinger equation

$$i \frac{\partial \psi}{\partial t} = -\frac{1}{2} \frac{\partial^2 \psi}{\partial x^2} - \frac{1}{2} \frac{\partial^2 \psi}{\partial y^2} + V \psi \quad (3)$$

(units $\hbar = 1$).

In de Broglie-Bohm theory, the particle traces out a definite trajectory $(x(t), y(t))$, which is determined by the wave function ψ according to the de Broglie guidance law

$$\frac{d\mathbf{x}}{dt} = \text{Im} \frac{\nabla\psi}{\psi} = \nabla S \quad (4)$$

(where $\psi = |\psi|e^{iS}$). Mathematically, $\text{Im}(\nabla\psi/\psi)$ is just the ratio of the quantum probability current to the quantum probability density. Physically, however, ψ is here interpreted as an objective field (in configuration space), guiding the motion of a *single* system.

Indeed, so far we have said nothing about probabilities or ensembles, and the equations (3) and (4) define a deterministic dynamics for individual particles. Given the initial wave function $\psi(x, y, 0)$, (3) determines the wave function $\psi(x, y, t)$ at all times; and given the initial particle position $(x(0), y(0))$, (4) then determines the particle trajectory $(x(t), y(t))$ at all times.

For an ensemble of independent particles, each guided by the same wave function $\psi(x, y, t)$, we may define a density $\rho(x, y, t)$ of actual configurations (x, y) at time t . The guidance equation (4) defines a velocity field (\dot{x}, \dot{y}) , and for an ensemble of particles with the same wave function ψ the field (\dot{x}, \dot{y}) determines the evolution of any distribution $\rho(x, y, t)$ via the continuity equation

$$\frac{\partial\rho}{\partial t} + \frac{\partial(\rho\dot{x})}{\partial x} + \frac{\partial(\rho\dot{y})}{\partial y} = 0 \quad (5)$$

Because (3) implies the continuity equation

$$\frac{\partial|\psi|^2}{\partial t} + \frac{\partial(|\psi|^2\dot{x})}{\partial x} + \frac{\partial(|\psi|^2\dot{y})}{\partial y} = 0 \quad (6)$$

for $|\psi|^2$, the particular initial distribution $\rho(x, y, 0) = |\psi(x, y, 0)|^2$ evolves into $\rho(x, y, t) = |\psi(x, y, t)|^2$. The state of ‘quantum equilibrium’ is preserved by the dynamics.

Note that (5) determines the evolution of *any* initial distribution $\rho(x, y, 0)$, even if $\rho(x, y, 0) \neq |\psi(x, y, 0)|^2$. Given $\psi(x, y, 0)$, (3) determines $\psi(x, y, t)$ at all times, and (4) then determines the velocity field (\dot{x}, \dot{y}) at all times. Once the velocity field (\dot{x}, \dot{y}) is known everywhere, (5) may be integrated to yield $\rho(x, y, t)$ at all times, for any initial $\rho(x, y, 0)$.

Before we proceed, it is instructive to compare the above with the analogous classical Hamiltonian evolution on phase space. Classically, the trajectory $(q(t), p(t))$ of an individual system is determined by Hamilton’s equations

$$\dot{q} = \frac{\partial H}{\partial p}, \quad \dot{p} = -\frac{\partial H}{\partial q} \quad (7)$$

given the initial values (q_0, p_0) . These equations define a velocity field (\dot{q}, \dot{p}) on phase space, and for an ensemble of systems with the same Hamiltonian

H the field (\dot{q}, \dot{p}) determines the evolution of any distribution $\rho(q, p, t)$ via the continuity equation

$$\frac{\partial \rho}{\partial t} + \frac{\partial(\rho \dot{q})}{\partial q} + \frac{\partial(\rho \dot{p})}{\partial p} = 0 \quad (8)$$

which may be rewritten as

$$\frac{\partial \rho}{\partial t} + \{\rho, H\} = 0 \quad (9)$$

Because $\partial \dot{q} / \partial q = -\partial \dot{p} / \partial p$, a uniform initial distribution $\rho(q, p, 0) = \text{const.}$ (on the energy surface) remains uniform, $\rho(q, p, t) = \text{const.}$. The state of thermal equilibrium is preserved by the dynamics. While for a general (non-uniform) initial state $\rho(q, p, 0)$, the evolution $\rho(q, p, t)$ is obtained (in principle) by integrating (9).

It is known that in appropriate circumstances, the classical evolution on phase space defined by (9) leads to thermal relaxation on a coarse-grained level (see Sect. 5 below). Less is known about the corresponding evolution (on configuration space) defined by (5).

Classically, the canonical example of thermal relaxation (for an isolated system) is that of a simple initial distribution $\rho(q, p, 0)$ (with no fine-grained microstructure) concentrated on a small region of the energy surface. Under the Hamiltonian evolution (9), the distribution $\rho(q, p, t)$ will generally develop a complex filamentary structure that spreads out over the energy surface, so that the distribution approaches uniformity on a coarse-grained level.

Here, we shall consider an analogous example, of particles in a two-dimensional box with a simple initial distribution $\rho(x, y, 0) \neq |\psi(x, y, 0)|^2$ (with no fine-grained microstructure). We shall see, by numerical integration of (5), that the ensemble evolves towards the equilibrium distribution $|\psi|^2$ (on a coarse-grained level).

Consider, then, a particle confined to a square box of side π , with infinite barriers at $x, y = 0, \pi$. The energy eigenfunctions are

$$\phi_{mn}(x, y) = \frac{2}{\pi} \sin(mx) \sin(ny) \quad (10)$$

with energy eigenvalues $E_{mn} = \frac{1}{2}(m^2 + n^2)$, where $m, n = 1, 2, 3, \dots$ are positive integers.

As a specific example, we take the initial wave function $\psi(x, y, 0)$ at $t = 0$ to be a superposition of the first 16 modes, $m, n = 1, 2, 3, 4$, with amplitudes of equal modulus but randomly-chosen phases θ_{mn} :⁵

$$\psi(x, y, 0) = \sum_{m,n=1}^4 \frac{1}{4} \phi_{mn}(x, y) \exp(i\theta_{mn}) \quad (11)$$

The squared-amplitude $|\psi(x, y, 0)|^2$ is shown in Fig. 1.

⁵For the record, the values of θ_{mn} used were (to four decimals) $\theta_{11} = 5.1306$, $\theta_{12} = 2.0056$, $\theta_{13} = 4.1172$, $\theta_{14} = 3.3871$, $\theta_{21} = 6.2013$, $\theta_{22} = 4.6598$, $\theta_{23} = 1.8770$, $\theta_{24} = 4.3033$, $\theta_{31} = 4.0145$, $\theta_{32} = 6.1142$, $\theta_{33} = 5.4401$, $\theta_{34} = 1.9292$, $\theta_{41} = 3.4015$, $\theta_{42} = 6.2109$, $\theta_{43} = 6.0370$, $\theta_{44} = 5.9159$.

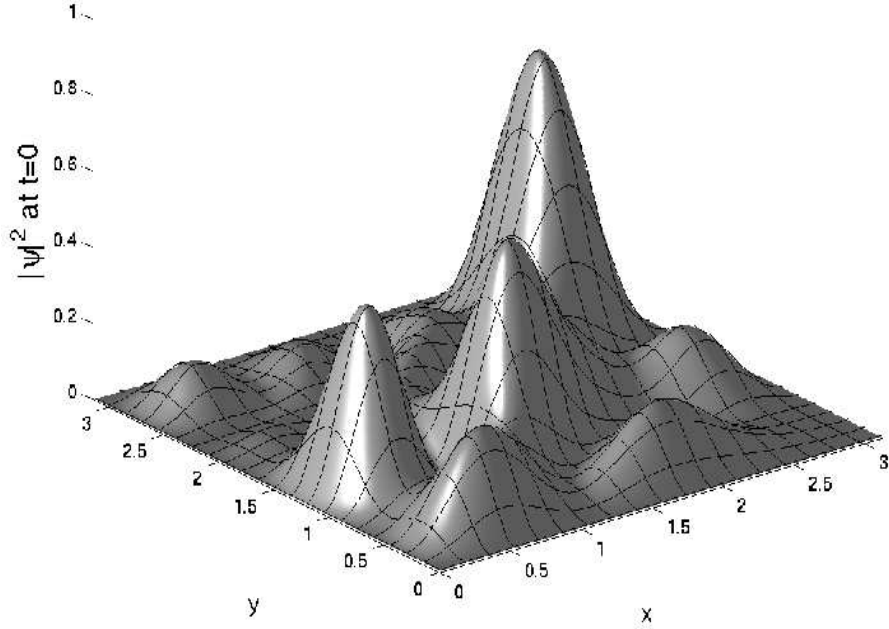


Figure 1: The squared-amplitude $|\psi(x, y, 0)|^2$ at $t = 0$, for the specified superposition of the first 16 modes of a two-dimensional box.

From (3), the wave function $\psi(x, y, t)$ at later times is just

$$\psi(x, y, t) = \sum_{m,n=1}^4 \frac{1}{4} \phi_{mn}(x, y) \exp i(\theta_{mn} - E_{mn}t) \quad (12)$$

Note that ψ is periodic in time, with period 4π (since $4\pi E_{mn}$ is always an integer multiple of 2π).

From (4), the velocity components of the particle at any moment are given by

$$\frac{dx}{dt} = \frac{i}{2|\psi|^2} \left(\psi \frac{\partial \psi^*}{\partial x} - \psi^* \frac{\partial \psi}{\partial x} \right) \quad (13)$$

and

$$\frac{dy}{dt} = \frac{i}{2|\psi|^2} \left(\psi \frac{\partial \psi^*}{\partial y} - \psi^* \frac{\partial \psi}{\partial y} \right) \quad (14)$$

3 Character of the Trajectories

The velocities (13) and (14) are ill-defined at nodes (where $|\psi| = 0$), and tend to diverge as nodes are approached. This is because, close to a node, small displacements in x and y can generate large changes in phase $S = \text{Im} \ln \psi$, corresponding to a large gradient ∇S .⁶ Note, however, that as shown by Berndt *et al.* [18, 19], for reasonable Hamiltonians and wave functions the set of initial particle positions that reach singularities of the velocity field in finite time is of $|\psi|^2$ -measure zero.

Thus, for almost all initial values $(x(0), y(0))$, the trajectory $(x(t), y(t))$ of the particle may be calculated by numerical integration of (13) and (14).

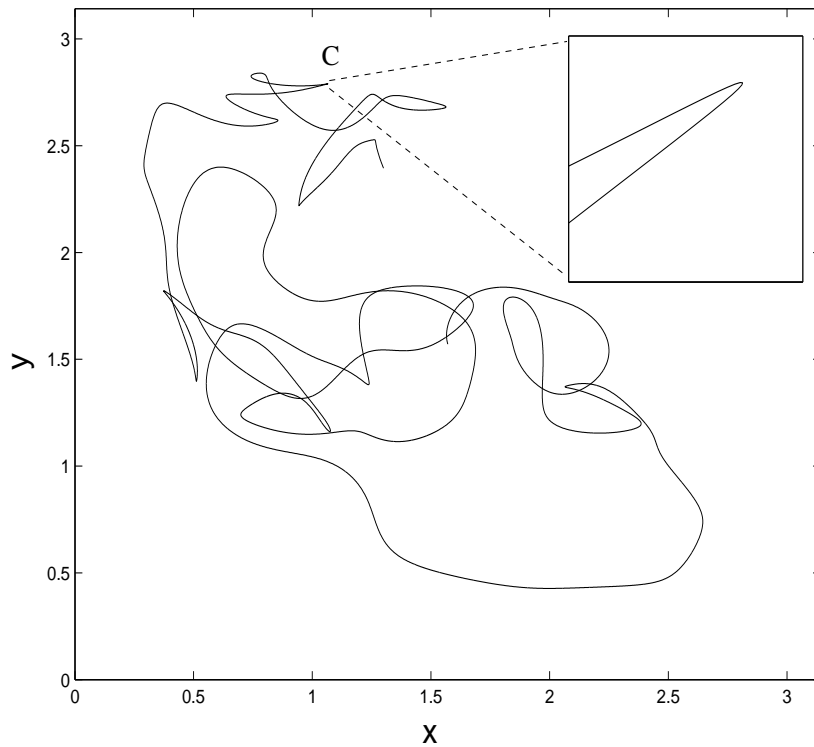


Figure 2: A typical trajectory, with an apparent cusp at C. The particle actually turns around very slowly at C.

Our method is based on the Runge-Kutta-Fehlberg algorithm [20], with an adaptive time step h adjusted so that the absolute errors in $x(t)$ and $y(t)$ at

⁶Because ψ is a smooth, single-valued function, a small displacement $(\delta x, \delta y)$ produces a small change $\delta\psi$ in the complex plane. However, close to a node ($|\psi| = 0$), $\delta\psi$ lies near the origin of the complex plane and so can correspond to a large change δS of phase.

each step are both less than $h\Delta$ for some fixed Δ . For each trajectory, we begin by setting $\Delta = 10^{-6}$. We then recalculate the same trajectory with $\Delta = 10^{-7}$. If the global error (the distance between the final positions) is less than 0.01, we retain the more accurate result. Otherwise, we recalculate with $\Delta = 10^{-8}$, and so on.

For a small number of trajectories, an accurate calculation was beyond the bounds of our computational resources, which we fixed at a minimum of $\Delta = 10^{-12}$ and a maximum of 10^8 time steps (per trajectory). Over a time 2π the number of problematic trajectories is about 1 in 60,000, while over a time 4π it is about 1 in 1,500 (sampling uniformly over the box).

A typical trajectory is shown in Fig. 2. In general, the trajectories are rather irregular.

At some points, for example at C (Fig. 2), there is an apparent cusp, but closer examination shows that the tangent to the curve is not discontinuous. Further, at least in this case, the velocity field at C is in fact very small: the particle is slowly turning around, with a speed in the range $\sim 10^{-2} - 10^{-3}$.

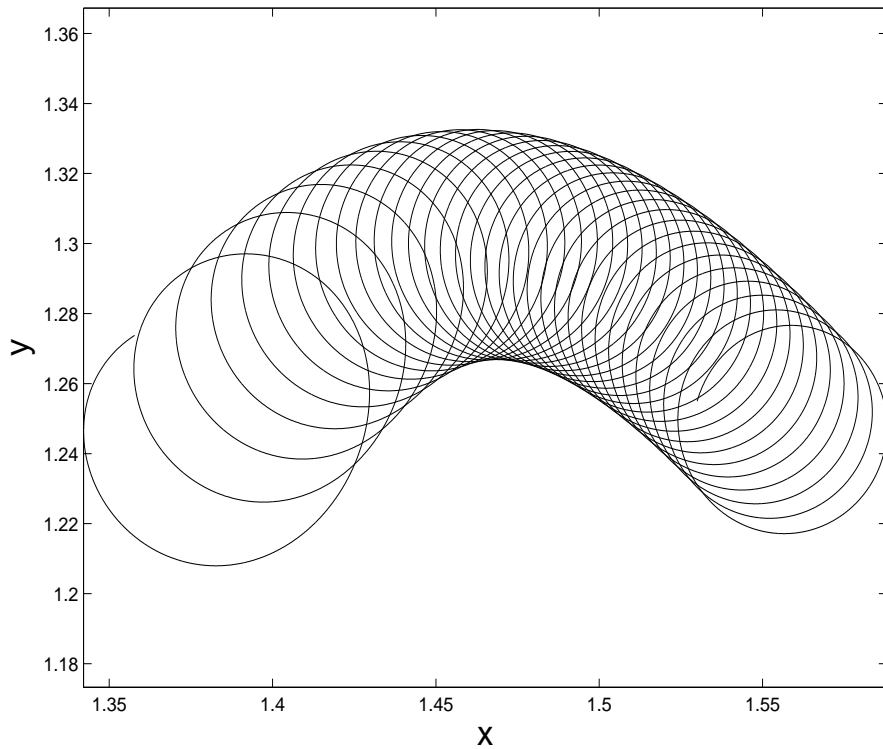


Figure 3: Close-up of a trajectory near a node or quasi-node (where $|\psi|$ is known to be very small and possibly zero). The particle rapidly circles around a moving point at which $1/|\psi|$ is highly peaked.

The motion tends to be particularly rapid in regions where $|\psi|$ is small. Fig. 3 shows a close-up of a trajectory near a nodal or quasi-nodal point, where $|\psi|$ is known to be very small (but not known to be strictly zero, it being impossible to tell in a numerical analysis). The spatial region shown is about 0.3% of the area of the whole box, and the displayed trajectory covers a time interval $\Delta t = 0.23$.⁷ The particle follows a rapid circular motion around a point moving from right to left in the figure – and the moving point is a node or quasi-node, at which $1/|\psi|$ is highly peaked. For the case shown, $1/|\psi|$ has an apparent peak value of about 60, and the speed of the particle varies widely from ~ 10 to ~ 50 .

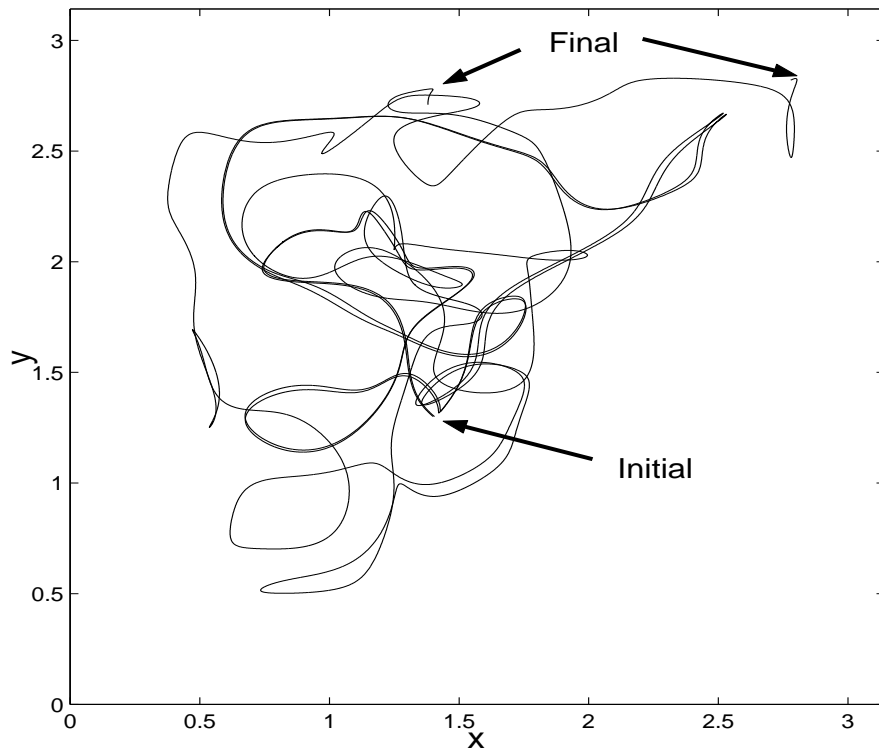


Figure 4: Illustration of the divergence of neighbouring trajectories.

In Fig. 4, we illustrate the divergence of neighbouring trajectories. Two distinct but nearby initial positions at $t = 0$ evolve after time $t = 4\pi$ into widely-separated final positions. For the example shown, the initial distance between the points is 0.005, while the final distance is 1.403.

The divergence of neighbouring trajectories and the behaviour of Lyapunov exponents in pilot-wave dynamics has been studied by a number of authors

⁷The region shown is $x \in (1.35, 1.6)$, $y \in (1.21, 1.33)$, and the time interval is $t \in (9.39, 9.62)$.

[21, 22, 23, 24]. Chaotic trajectories have been reported for a range of systems: the two-dimensional anisotropic harmonic oscillator [21, 22], the quantum kicked rotor [23, 25], the quantum cat map [26], the hydrogen atom in an external field [27], the Hénon-Heiles oscillator [28], and a two-particle stationary state [29].

For the two-dimensional square box, chaotic trajectories have been reported by Frisk [24], who emphasises the importance of nodes in generating chaotic motion, and whose numerical simulations suggest a proportionality between the Lyapunov exponent and the number of nodes.

4 Relaxation to Quantum Equilibrium

We now turn to the time evolution of an initial nonequilibrium ensemble. We assume that every particle in the ensemble is guided by the same wave function $\psi(x, y, t)$, given by (12). At $t = 0$, the (nonequilibrium) distribution is chosen to be

$$\rho(x, y, 0) = \left(\frac{2}{\pi}\right)^2 \sin^2 x \sin^2 y \quad (15)$$

This is just $|\phi_{11}(x, y)|^2$ – that is, the ground-state equilibrium distribution. It is displayed in Fig. 5.

Instead of integrating the continuity equation (5) directly, it is more convenient to calculate the trajectories, from which it is straightforward to deduce the evolution of any initial distribution $\rho(x, y, 0)$.

From (5) and (6), it follows that the ratio

$$f(x, y, t) \equiv \frac{\rho(x, y, t)}{|\psi(x, y, t)|^2} \quad (16)$$

is conserved along trajectories: $df/dt = 0$ or

$$\frac{\partial f}{\partial t} + \frac{dx}{dt} \frac{\partial f}{\partial x} + \frac{dy}{dt} \frac{\partial f}{\partial y} = 0$$

If the initial point (x_0, y_0) evolves into (x, y) at time t , then for any ensemble

$$f(x, y, t) = f(x_0, y_0, 0) \quad (17)$$

Thus, given the function

$$f(x_0, y_0, 0) = \frac{\rho(x_0, y_0, 0)}{|\psi(x_0, y_0, 0)|^2}$$

at $t = 0$, the distribution $\rho(x, y, t)$ at later times may be written as

$$\rho(x, y, t) = |\psi(x, y, t)|^2 f(x_0, y_0, 0) \quad (18)$$

Given the mapping from (x_0, y_0) to (x, y) , the fate of any initial distribution $\rho(x, y, 0)$ may be deduced from (18).

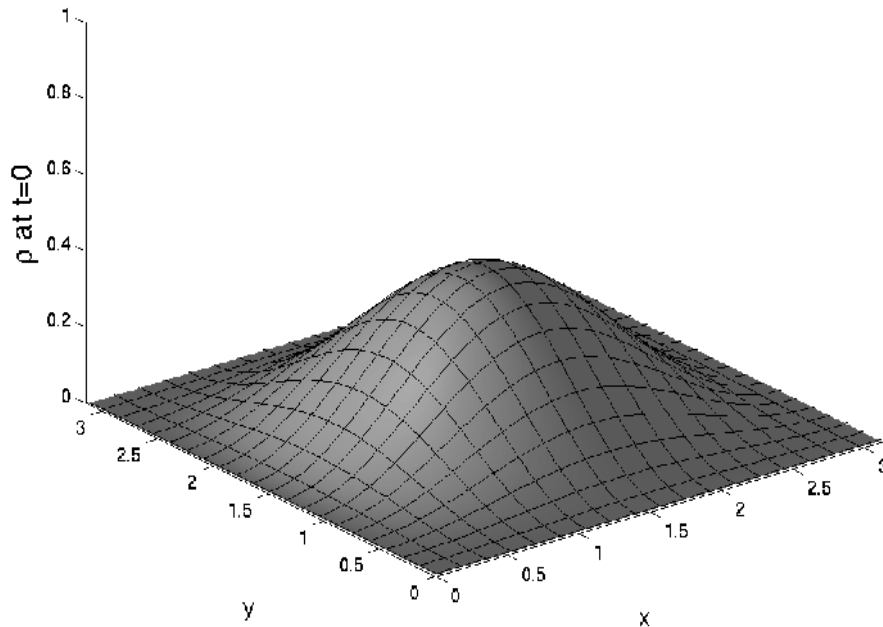


Figure 5: The initial nonequilibrium distribution, chosen to be $\rho(x, y, 0) = |\phi_{11}(x, y)|^2$ (equal to the ground-state equilibrium distribution).

One might begin with a uniform lattice of initial points (x_0, y_0) , and calculate the future trajectories $(x(t), y(t))$, using (18) to deduce the distribution $\rho(x(t), y(t), t)$ at the later points $(x(t), y(t))$. This method was used in the first relaxation simulation, for the simple case of a one-dimensional box [4]. However, the lattice of points at later times is unfortunately distorted, and there appear large regions containing hardly any lattice points at all.

A more accurate procedure is to evolve trajectories *backwards*, from (x, y) at any desired t to the starting point (x_0, y_0) at $t = 0$ [30]. Thus, to calculate $\rho(x, y, t)$ at time t , we set up a uniform lattice of points (x, y) at time t and backtrack the trajectories to the initial points (x_0, y_0) at $t = 0$. Knowing the function $f(x_0, y_0, 0)$, we may then use (18) to deduce $\rho(x, y, t)$.

This backtracking procedure has the disadvantage that one has to calculate the trajectories over the whole interval from t to $t = 0$, for every desired value of t (for which one wishes to know $\rho(x, y, t)$). But overall the procedure is better, because it generates results for $\rho(x, y, t)$ on a uniform lattice. This is particularly important when one wishes to calculate the coarse-grained H -function.

As mentioned in Sect. 3, for some trajectories an accurate calculation is beyond our computational resources ($\Delta = 10^{-12}$ and 10^8 time steps per trajectory). Nevertheless, for practical reasons of data handling, it is convenient to assign values to all of them, rather than ignore the problematic cases.⁸ Since the number of problematic trajectories is found to be small (1 in 60,000 over a time 2π and 1 in 1,500 over a time 4π), they have a negligible effect on the results reported below.

Note that because the values of $f = \rho/|\psi|^2$ are carried along trajectories, the exact (fine-grained) value of $\rho(x, y, t)$ will always differ from $|\psi(x, y, t)|^2$, by just the same multiplicative factor $f(x_0, y_0, 0)$ by which $\rho(x_0, y_0, 0)$ differed from $|\psi(x_0, y_0, 0)|^2$. Indeed, the property $df/dt = 0$ is analogous to the Liouville property in classical statistical mechanics, according to which the phase-space density is constant along Hamiltonian trajectories (see Sect. 5 below). In both cases, relaxation occurs only in a coarse-grained sense.

To see how this works, in Fig. 6 we show a close-up of $\rho(x, y, t)$ in a small fixed region of the box, at time $t = \pi$. The exact, fine-grained distribution is highly irregular. The area shown is very small: it has side $\pi/128$, covering just 0.006% of the total area of the box. (For this calculation, we used a uniform lattice of 40,000 points in this small area, with the lattice specified at $t = \pi$.)

Clearly, the exact fine-grained distribution is extremely complex, and it is useful to consider its appearance under coarse-graining. Given a (square) coarse-graining cell of side ε , the distribution ρ may be averaged over the cell to produce a coarse-grained value

$$\frac{1}{\varepsilon^2} \int \int_{\text{cell}} dx dy \rho \quad (19)$$

which may be assigned to the centre of the cell.

If the cells do not overlap, we denote the coarse-grained distribution by $\bar{\rho}$. Results for $\bar{\rho}$ will be shown in Sect. 5 below (using a coarse-graining length $\varepsilon = \pi/32$).

A smoother coarse-grained distribution, denoted $\tilde{\rho}$, is obtained if one takes overlapping cells (a procedure used in quantum chemistry, for example). To generate $\tilde{\rho}$, we take cells of side $\varepsilon = \pi/16$ that overlap with their immediate neighbours in 88% of their area. Specifically, given one cell, shifting it along x or y by a distance equal to 12% of its length (that is, 12% of $\pi/16$) generates the neighbouring cell, and so on. In this way, in the box of area π^2 we obtain a patchwork of 126×126 overlapping cells, each with its own value of $\tilde{\rho}$. For the trajectory calculations, we use a lattice of 400×400 particles, with 25×25 particles in each cell.

We have calculated the evolution of $\tilde{\rho}$ up to $t = 4\pi$ (when $|\psi|^2$ recurs to its initial value). This is shown in Fig. 7. Displayed are $\tilde{\rho}$ and $|\psi|^2$, at times

⁸Some cases required more than 10^8 time steps even for $\Delta = 10^{-6}$; each of these were aborted and assigned a value from a neighbouring trajectory. In other cases, decreasing Δ exceeded the limit of 10^8 time steps, and we retained the value obtained using the smallest value of Δ that did not exceed this limit (despite the global error exceeding 0.01). Finally, some cases reached the minimum setting $\Delta = 10^{-12}$ without achieving the desired limit on the global error, and for these we assigned the value obtained using $\Delta = 10^{-12}$.

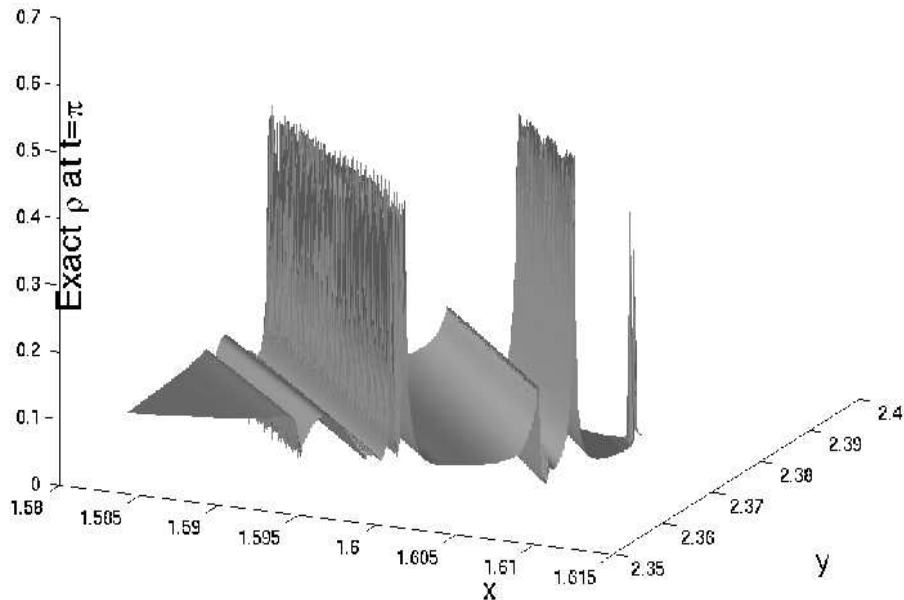


Figure 6: Close-up of the exact $\rho(x, y, t)$ in a small spatial region, covering just 0.006% of the area of the box, at time $t = \pi$. The fine-grained distribution is very irregular.

$t = 0, 2\pi$ and 4π . Evidently, $\tilde{\rho}$ and $|\psi|^2$ become rather close, and a remarkable relaxation towards quantum equilibrium has occurred after just one time cycle of 4π .

Fig. 8 shows the same data, as contour plots.

Note that while ψ and its associated velocity field are periodic, in general the trajectories are not, so that the distribution ρ does *not* recur at $t = 4\pi$. This is in contrast with the one-dimensional case, where the particles cannot move past each other, constraining each trajectory to recur simultaneously with $|\psi|^2$, so that any initial $\rho_0 \neq |\psi_0|^2$ recurs as well [4, 17].

Presumably, evolution over more time cycles of 4π will make $\tilde{\rho}$ converge ever closer to $|\psi|^2$. However, we have not extended our calculations beyond $t = 4\pi$. Possibly, a small residual nonequilibrium will remain after an arbitrary number of cycles, but this seems unlikely.

Given the mapping from (x_0, y_0) to $(x(4\pi), y(4\pi))$, not only can one immediately construct $\rho(x, y, 4\pi)$ from any initial $\rho(x, y, 0)$, one can also extend

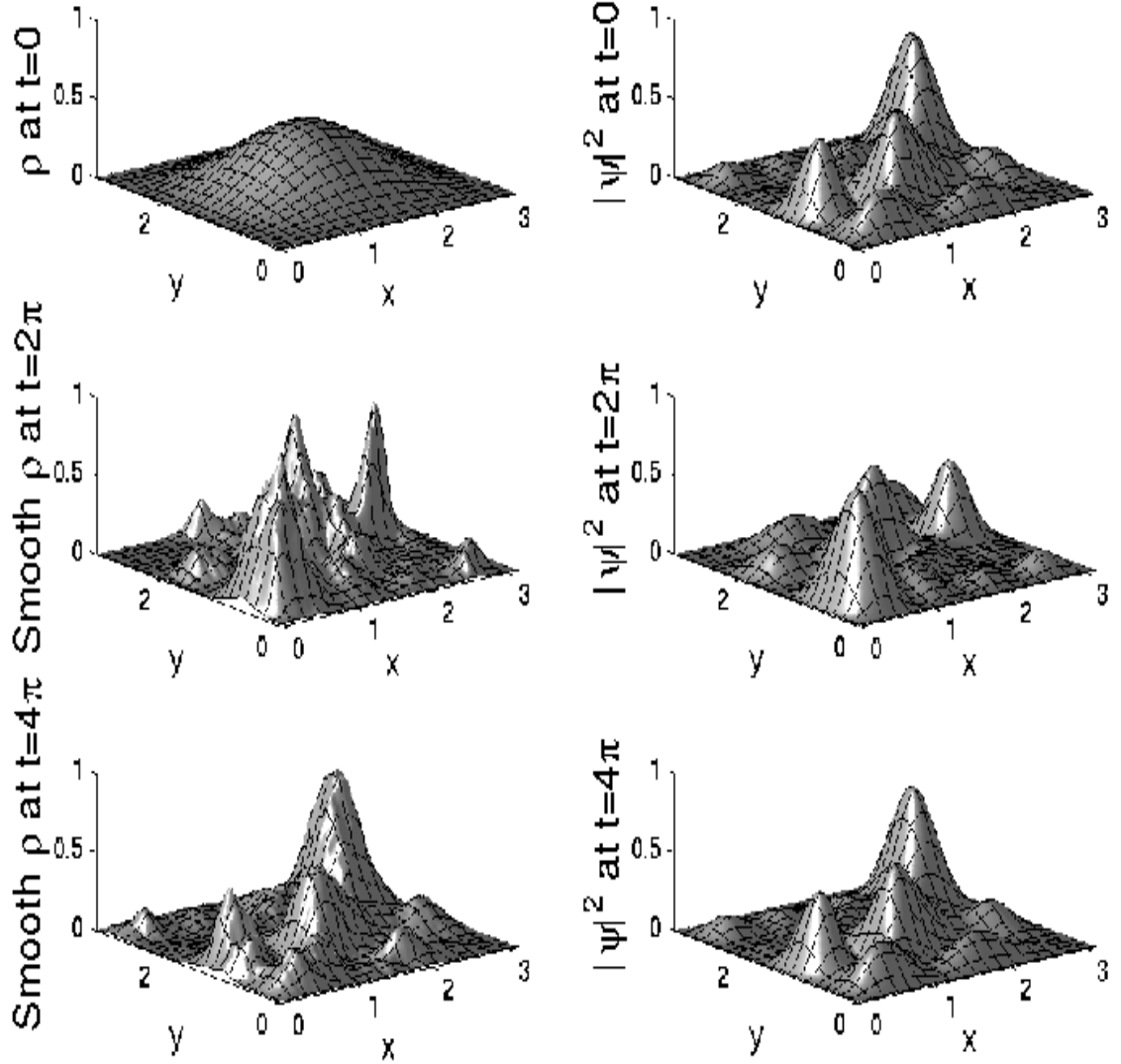


Figure 7: Smoothed $\bar{\rho}$, compared with $|\psi|^2$, at times $t = 0, 2\pi$ and 4π . While $|\psi|^2$ recurs to its initial value, the smoothed $\bar{\rho}$ shows a remarkable evolution towards equilibrium.

the evolution to an arbitrary number of cycles 4π – that is, to times $t = 4\pi n$ for positive integral n – by simple iteration of the mapping (the velocity field being periodic with period 4π). It might then appear that, given the calcula-

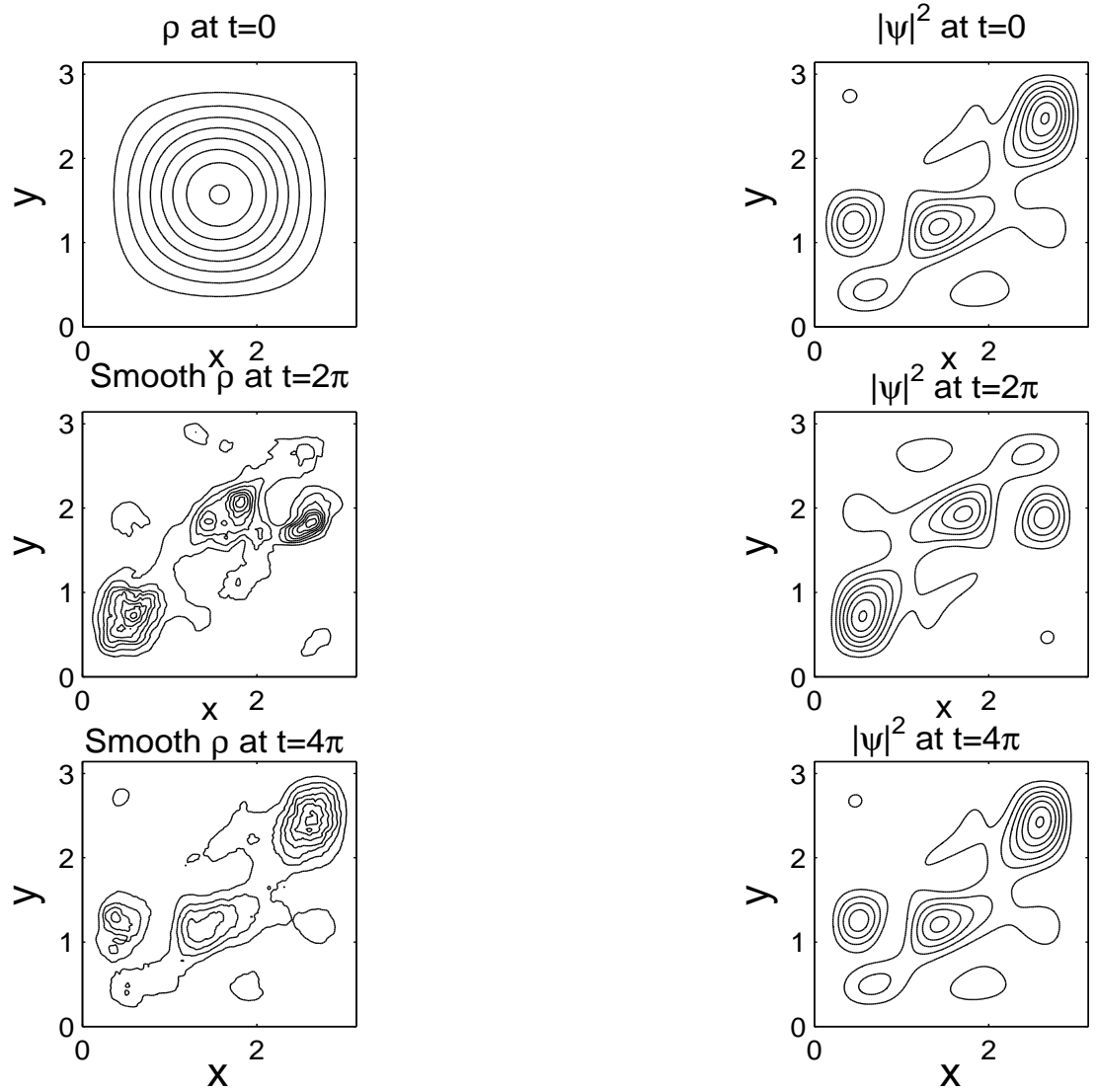


Figure 8: Smoothed $\tilde{\rho}$, compared with $|\psi|^2$, at times $t = 0, 2\pi$ and 4π . The same data as in Fig. 8, displayed as contour plots.

tions performed so far, we could easily extend them to $t = 4\pi n$. Unfortunately, the calculated map from (x_0, y_0) to $(x(4\pi), y(4\pi))$ cannot be reapplied to map $(x(4\pi), y(4\pi))$ to $(x(8\pi), y(8\pi))$ and so on, because the backtracking method we have used distorts the lattice at $t = 0$.

5 Decay of the H -Function; Relaxation Timescale

The difference between ρ and $|\psi|^2$ may be quantified by the value of the H -function (1). As we mentioned in the Introduction, this is just minus the relative entropy of ρ with respect to $|\psi|^2$ (a standard measure of the difference between two distributions). The H -function is bounded below by zero, and is equal to zero if and only if $\rho = |\psi|^2$ everywhere [16, 4, 17].

Note, however, that because of (5) and (6) the exact H is constant in time, $dH/dt = 0$, reflecting the fact (already mentioned) that differences between fine-grained values of ρ and $|\psi|^2$ never disappear (the ratio $f = \rho/|\psi|^2$ being carried along trajectories). A decreasing H is obtained only under coarse-graining.

The situation is similar classically, where departures from thermal equilibrium may be quantified in terms of the classical H -function (on phase space)

$$H_{\text{class}} = \int \int dqdp \rho \ln \rho$$

which is just minus the relative entropy of ρ with respect to the uniform distribution. Under Hamiltonian evolution, $d\rho/dt = 0$ along trajectories (Liouville's theorem), and the exact H_{class} is constant, $dH_{\text{class}}/dt = 0$. However, in appropriate circumstances, the classical phase-space evolution defined by (9) leads to thermal relaxation on a coarse-grained level. This may be quantified in terms of the classical coarse-grained H -function

$$\bar{H}_{\text{class}} = \int \int dqdp \bar{\rho} \ln \bar{\rho}$$

where $\bar{\rho}$ is ρ averaged over (non-overlapping) coarse-graining cells. This obeys the coarse-graining H -theorem [31, 32]

$$\bar{H}_{\text{class}}(t) \leq \bar{H}_{\text{class}}(0)$$

(assuming no initial fine-grained microstructure in ρ at $t = 0$), and \bar{H}_{class} is minimised by $\bar{\rho} = \text{const.}$. This theorem formalises the intuitive idea of Gibbs – that an initial non-uniform distribution will tend to develop fine-grained structure and become more uniform on a coarse-grained level.

In the pilot-wave case too, the evolution (on configuration space) may lead to relaxation on a coarse-grained level, as shown by the above numerical simulations. And the relaxation may be similarly quantified in terms of the coarse-grained H -function

$$\bar{H} = \int dq \bar{\rho} \ln(\bar{\rho}/\overline{|\psi|^2}) \tag{20}$$

which obeys the H -theorem [16, 4, 17]

$$\bar{H}(t) \leq \bar{H}(0)$$

(assuming no initial fine-grained microstructure in ρ and $|\psi|^2$), and where again $\bar{H} \geq 0$ for all $\bar{\rho}$, $\overline{|\psi|^2}$ and $\bar{H} = 0$ if and only if $\bar{\rho} = \overline{|\psi|^2}$ everywhere. This

version of the H -theorem formalises the idea that ρ and $|\psi|^2$ behave like two ‘fluids’ which are ‘stirred’ by the same velocity field (since they obey the same continuity equation), so that ρ and $|\psi|^2$ tend to become indistinguishable on a coarse-grained level.⁹

A natural timescale τ for relaxation may be defined in terms of the time derivatives of $\bar{H}(t)$ at $t = 0$.

Using the continuity equations (5) and (6), it follows that $(d\bar{H}/dt)_0 = 0$ and (for $q = (x, y)$) [4]

$$\left(\frac{d^2\bar{H}}{dt^2}\right)_0 = - \int \int dx dy \frac{|\psi_0|^2}{f_0} \left(\overline{(\dot{X}_0 \cdot \nabla f_0)^2} - \overline{(\dot{X}_0 \cdot \nabla f_0)}^2 \right) \leq 0 \quad (21)$$

where $\psi_0 = \psi(x, y, 0)$, $f_0 = f(x, y, 0)$, $\dot{X}_0 \equiv (\dot{x}_0, \dot{y}_0)$ and $\nabla \equiv (\partial/\partial x, \partial/\partial y)$. (The quantity in brackets is non-negative, and is equal to the spatial variance of $\dot{X}_0 \cdot \nabla f_0$ over a coarse-graining cell.)

Thus we may define τ by [4]

$$\frac{1}{\tau^2} \equiv - \frac{(d^2\bar{H}/dt^2)_0}{H_0} \quad (22)$$

where (21) gives $(d^2\bar{H}/dt^2)_0$ in terms of the initial conditions ψ_0 and ρ_0 .

Expanding $\dot{X}_0 \cdot \nabla f_0$ in a Taylor series within each coarse-graining cell of area ε^2 , it is found that

$$(d^2\bar{H}/dt^2)_0 = -\frac{\varepsilon^2}{12} I + O(\varepsilon^4) \quad (23)$$

where [17, 10]

$$I \equiv \int \int dx dy \frac{|\psi_0|^2}{f_0} |\nabla(\dot{X}_0 \cdot \nabla f_0)|^2 \quad (24)$$

Thus

$$\tau = \frac{1}{\varepsilon} \sqrt{\frac{12H_0}{I}} + O(\varepsilon) \quad (25)$$

If ε is small with respect to the lengthscale over which $\dot{X}_0 \cdot \nabla f_0$ varies, then $\tau \propto 1/\varepsilon$. Taking $H_0 \sim 1$ (a mild nonequilibrium), a rough estimate of I yields the quoted result (2), in terms of the quantum energy spread ΔE of ψ_0 [17, 10].

Note that, given the result $\tau \propto 1/\varepsilon$ (for small ε), the formula (2) may be obtained on dimensional grounds. And in any case, (2) is only a rough, order-of-magnitude estimate. For our initial wave function (11), $\Delta E \simeq 4$ and (in our units)

$$\tau \sim \frac{1}{8\varepsilon} \quad (26)$$

Thus, at least initially, $\bar{H} = \bar{H}(t)$ should decay on a timescale of order $1/8\varepsilon$.

⁹Note, however, that the velocity field (4) is related to ψ by the Schrödinger equation, as well as by the continuity equation, whereas no such additional relation exists between the velocity field and ρ . This explains why ρ develops a filamentary structure while $|\psi|^2$ does not [4].

To investigate the decay of $\overline{H}(t)$ numerically, we must work in terms of the coarse-grained quantities $\bar{\rho}$ and $\overline{|\psi|^2}$, with non-overlapping coarse-graining cells (as used in the above H -theorem).

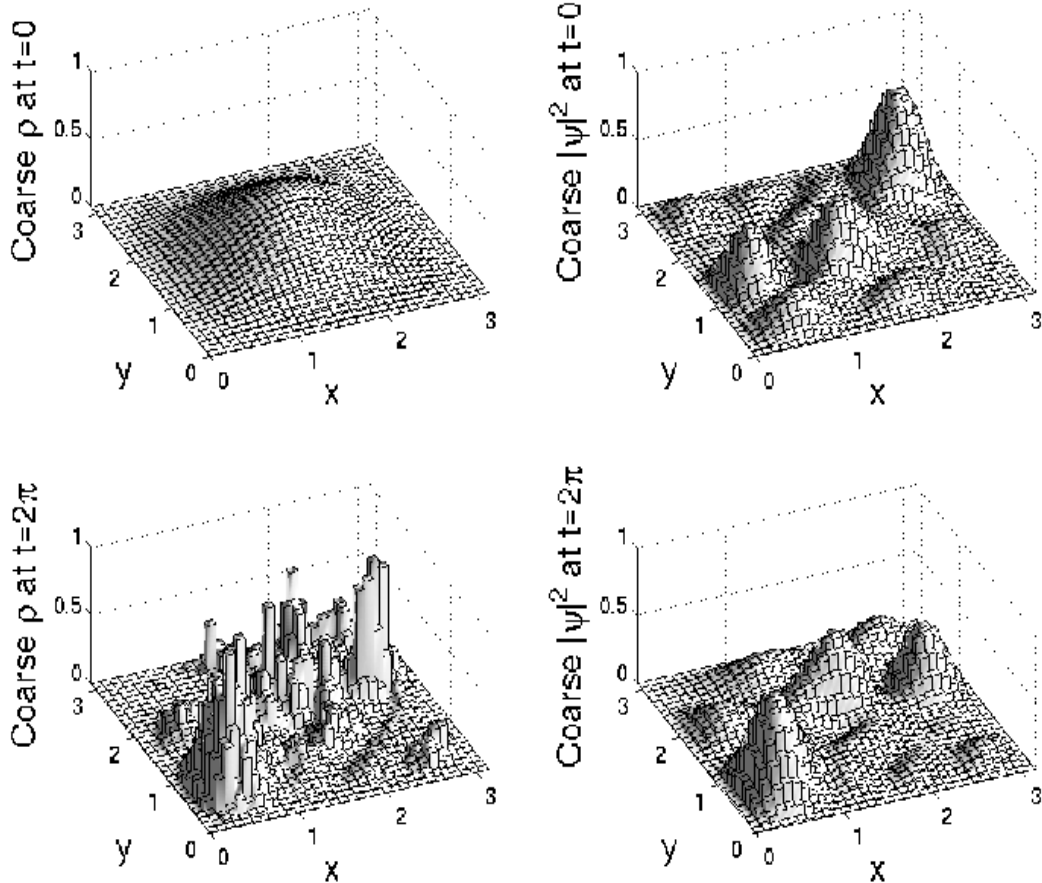


Figure 9: Coarse-grained $\bar{\rho}$ and coarse-grained $\overline{|\psi|^2}$ (with non-overlapping cells) at times $t = 0$ and $t = 2\pi$.

Fig. 9 displays $\bar{\rho}$ and $\overline{|\psi|^2}$, with non-overlapping cells of side $\varepsilon = \pi/32$, at times $t = 0$ and $t = 2\pi$.

In Fig. 10, we plot $\ln \bar{H}$ against time from $t = 0$ to $t = 2\pi$ (where the value of \bar{H} was calculated every $\pi/4$ time units). The evolution of $\ln \bar{H}$ is approximately linear, corresponding to an approximately exponential decay $\bar{H}(t) \approx \bar{H}_0 e^{-t/t_c}$, with a (best-fitting) time constant $t_c \approx 4$. This compares favourably with the order-of-magnitude estimate (26), which for the present coarse-graining length $\varepsilon = \pi/32$ gives $\tau \sim 1.3$.

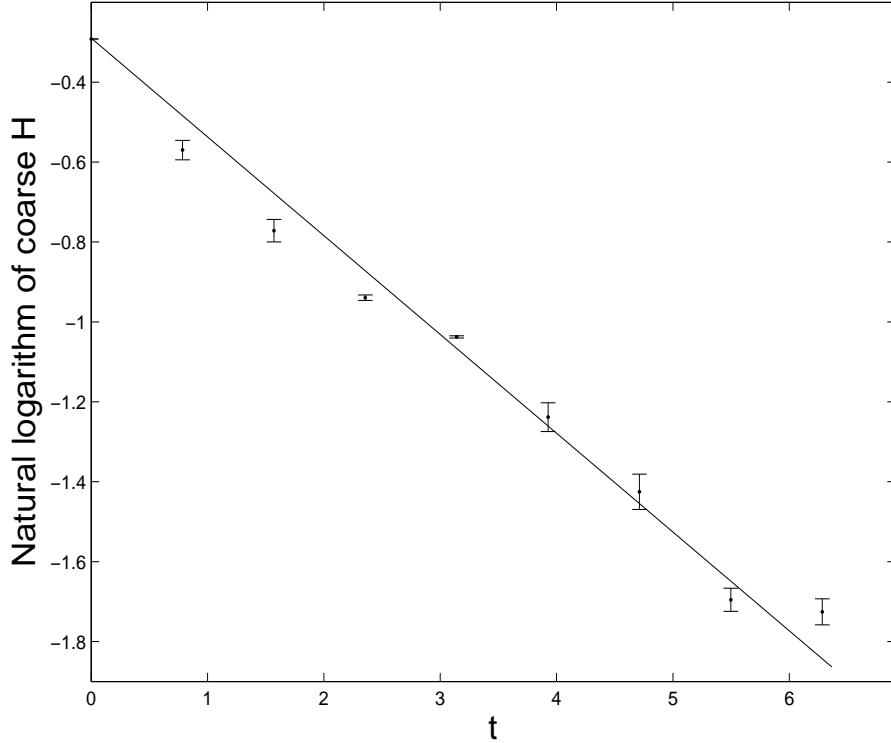


Figure 10: Plot of $\ln \bar{H}$ against time, from $t = 0$ to $t = 2\pi$, showing an approximately exponential decay of $\bar{H}(t)$ with a time constant $t_c \approx 4$.

Fig. 10 shows error bars for the displayed values of $\ln \bar{H}$. These were obtained as follows. The main source of error is the approximation of $\bar{\rho}$ by an average over a finite number of points within a coarse-graining cell. To estimate this error, each calculation of $\bar{\rho}$ is done again with a different lattice of points, corresponding to a different sampling within the cells (first with a lattice of 25×25 particles, then with 27×27). The two results yield different values for \bar{H} ; however, the difference is usually only about 2%, and never more than 4%. Another (considerably smaller) source of error in \bar{H} is of course the inaccuracy in the calculated particle positions. This error is estimated by comparing values of \bar{H} obtained with local errors Δ (in the trajectories) differing by a factor of ten; the difference in values of \bar{H} is found to be quite negligible.

Note that the natural quantum timescale for this system is $\Delta t \sim \hbar/\Delta E \sim 0.25$, which is arguably not much further from t_c than is τ . However, generally speaking, the quantum timescale $\Delta t \sim \hbar/\Delta E$ for a system is unrelated to the estimated relaxation timescale $\tau \sim (1/\varepsilon)\hbar^2/m^{1/2}(\Delta E)^{3/2}$ in (2), since Δt has no dependence on ε and scales differently with ΔE . Writing $\Delta E \sim (\Delta p)^2/2m$,

the special choice of $\varepsilon \sim \hbar/\Delta p$ for the coarse-graining length leads to $\tau \sim \Delta t$, and our estimated τ is not far from Δt only because our ε is not far from $\hbar/\Delta p$.

It would be interesting to check numerically the dependence of the relaxation timescale on the coarse-graining length ε and on the energy spread ΔE . This has been done for the rather artificial but much simpler case of the one-dimensional box (in which trajectories cannot move past each other), with results that accord quite well with the predicted scalings $\tau \propto 1/\varepsilon$ and $\tau \propto 1/(\Delta E)^{3/2}$ [17, 33]. To perform the corresponding checks for the two-dimensional case is a task for the future.

We have found an approximately exponential decay of \bar{H} with time. Presumably this behaviour could be derived, by supplementing the underlying dynamics with some sort of phenomenological Markovian assumption, analogous to the classical hypothesis of molecular chaos at every instant (from which the Boltzmann equation may be derived).

6 Discussion and Conclusion

We have seen that the simple choice of an initial nonequilibrium state (15) relaxes towards equilibrium rather efficiently, with an accompanying (approximately exponential) decrease in the coarse-grained H -function on the expected timescale.

Of course, this is not to imply that *any* initial distribution $\rho_0 \neq |\psi_0|^2$ would relax to equilibrium: that is impossible in any time-reversal invariant theory. Just as in classical mechanics, for every solution of the dynamical laws evolving towards equilibrium, there is a time-reversed solution evolving away from equilibrium. For example, as new initial conditions ψ'_0, ρ'_0 at $t = 0$ we could take

$$\psi'(x, y, 0) = \psi^*(x, y, \pi), \quad \rho'(x, y, 0) = \rho(x, y, \pi) \quad (27)$$

where $\rho(x, y, \pi)$ is the former (exact) distribution at $t = \pi$, whose complex fine-grained microstructure is shown in close-up in Fig. 6. The dynamical equations (3) and (5) imply that these conditions will evolve into

$$\psi'(x, y, t) = \psi^*(x, y, \pi - t), \quad \rho'(x, y, t) = \rho(x, y, \pi - t) \quad (28)$$

so that after a time $t = \pi$ we recover our former initial distribution $\rho(x, y, 0)$ given by (15) – which is further away from equilibrium than the present initial state (27). Thus the initial conditions (27) evolve away from equilibrium, and the coarse-grained H -function increases with time.

However, as in ordinary statistical mechanics, relaxation towards equilibrium will be obtained if one assumes that the initial state satisfies certain conditions – such as the absence of fine-grained microstructure – which are violated by time-reversed ‘initial’ states such as (27). Conceptually, the situation here is the same as in ordinary statistical mechanics.

Conceptual issues in statistical mechanics arguably reduce to issues about initial conditions, and these are inevitably bound up with questions of cosmology

[32, 34, 35, 36, 17]. According to our current understanding, we see thermal nonequilibrium in our universe today only because gravity has the remarkable property of amplifying small inhomogeneities in temperature and energy density, leading to the formation of large-scale structure out of a primordial homogeneous state of thermal equilibrium [37]. In the absence of gravity, a classical isolated system with no initial fine-grained structure would be expected to evolve towards thermal equilibrium, just as in pilot-wave dynamics.

Initial conditions can be questioned. A lot of current work in cosmology is motivated by the desire to explain, for example, why the early universe was so smooth and homogeneous, and the prevailing view is that the homogeneity arose from interactions taking place at even earlier times (within cosmological horizons). Similarly, in the de Broglie-Bohm formulation of quantum theory, one may ask why all physical systems probed so far follow the Born rule $\rho = |\psi|^2$. Because these systems all have a long and violent astrophysical history, it is reasonable to explain the distribution $\rho = |\psi|^2$ in terms of a relaxation process from an earlier nonequilibrium state $\rho \neq |\psi|^2$. This leads naturally to the suggestion that quantum nonequilibrium may have existed in the early universe, in which case the quantum noise we see today may be regarded as a remnant of the big bang [38, 4, 39, 17, 10]. A similar view may be taken in any deterministic hidden-variables theory [40, 41, 42].

In the original pilot-wave version of the H -theorem [16], it was argued that relaxation $P \rightarrow |\Psi|^2$ would occur (on a coarse-grained level) for an ensemble of many-body systems with distribution $P(\mathbf{x}_1, \mathbf{x}_2, \dots, \mathbf{x}_N, t)$ and wave function $\Psi(\mathbf{x}_1, \mathbf{x}_2, \dots, \mathbf{x}_N, t)$ (with N large). It was then shown that single particles extracted from the (eventual) equilibrium ensemble and prepared with wave function ψ would have a distribution $\rho = |\psi|^2$. However, it is now clear from the above simulations that a large number of degrees of freedom are not needed for efficient relaxation to occur. Even for a single particle, relaxation will occur rapidly if its wave function is a superposition of even a modest number of energy eigenfunctions, as our numerical example shows.

The simulations performed in this paper add substance to the view, already mentioned, that relaxation occurs because ρ and $|\psi|^2$ evolve like two ‘fluids’ which are ‘stirred’ by the same velocity field. The most efficient mixing is found to occur in the neighbourhood of nodes or quasi-nodes, where $|\psi|$ is small. These points move around inside the box, rather like ‘electric mixers’ (or stirring devices) moving through a fluid, generating an efficient relaxation everywhere.

We mentioned in Sect. 2 that the importance of nodes in generating chaotic motion was noted by Frisk [24]. Frisk also suggested that nodes would be important if the motion is to have the appropriate mixing properties required for complete relaxation to quantum equilibrium. The above simulations certainly bear out the expectation that nodes provide a particularly efficient mixing. But whether or not relaxation would take place even in their absence (perhaps on much longer timescales) is not known.

Many details remain to be understood. We are far from a full understanding of pilot-wave theory as a dynamical system. General properties of the flow, such as ergodicity and mixing (in a rigorous sense), remain to be investigated. Still,

the results already in hand strongly suggest that, in de Broglie-Bohm theory, the distribution $\rho = |\psi|^2$ is an equilibrium state quite analogous to thermal equilibrium in classical physics.

It should be noted that the status of the Born rule has been a contentious issue in quantum theory generally, perhaps most notably in the many-worlds formulation of Everett [43, 44, 45]. Some recent authors [46, 47] base their justification of the Born rule on Gleason's theorem [48], which states that the Born rule is the unique probability assignment satisfying 'noncontextuality' – the condition that the probability for an observable should not depend on which other (commuting) observables are simultaneously measured. However, as pointed out by Bell [49], Gleason's noncontextuality condition is very strong, as it amounts to assuming that mutually-incompatible experimental arrangements yield the same statistics for the observable in question. Saunders [50] gives an 'operational' derivation of the Born rule (in which it is assumed that probabilities are determined by the quantum state alone); while Zurek [51] appeals to 'environment-assisted invariance'. Other recent derivations of the Born rule arise from novel axioms for quantum theory [52, 53].

Like Euclid's axiom of parallels in geometry, the Born rule seems to stand apart from the other axioms of quantum theory, and there have been a number of attempts to derive it either from the other axioms or from something else. We have argued in this paper that, in the de Broglie-Bohm formulation of quantum theory, the Born rule has a status similar to that of thermal equilibrium in ordinary statistical mechanics, and should not be regarded as an axiom at all.

Acknowledgement

We wish to thank Rickard Jonsson for assistance with the figures.

References

- [1] L. de Broglie, in: *Électrons et Photons: Rapports et Discussions du Cinquième Conseil de Physique*, ed. J. Bordet (Gauthier-Villars, Paris, 1928). [English translation: G. Bacciagaluppi and A. Valentini, *Electrons and Photons: The Proceedings of the Fifth Solvay Congress* (Cambridge University Press, Cambridge, forthcoming).]
- [2] D. Bohm, Phys. Rev. **85**, 166; 180 (1952).
- [3] J.S. Bell, *Speakable and Unsayable in Quantum Mechanics* (Cambridge University Press, Cambridge, 1987).
- [4] A. Valentini, On the Pilot-Wave Theory of Classical, Quantum and Subquantum Physics, PhD thesis, International School for Advanced Studies, Trieste, Italy (1992).

- [5] P. Holland, *The Quantum Theory of Motion: an Account of the de Broglie-Bohm Causal Interpretation of Quantum Mechanics* (Cambridge University Press, Cambridge, 1993).
- [6] D. Bohm and B.J. Hiley, *The Undivided Universe: an Ontological Interpretation of Quantum Theory* (Routledge, London, 1993).
- [7] J.T. Cushing, *Quantum Mechanics: Historical Contingency and the Copenhagen Hegemony* (University of Chicago Press, Chicago, 1994).
- [8] *Bohmian Mechanics and Quantum Theory: an Appraisal*, eds. J.T. Cushing, A. Fine, and S. Goldstein (Kluwer, Dordrecht, 1996).
- [9] D. Dürr, *Bohmsche Mechanik als Grundlage der Quantenmechanik* (Springer, 2001).
- [10] A. Valentini, *Pilot-Wave Theory of Physics and Cosmology* (Cambridge University Press, Cambridge, forthcoming).
- [11] W. Pauli, in: *Louis de Broglie: Physicien et Penseur* (Albin Michel, Paris, 1953).
- [12] J.B. Keller, Phys. Rev. **89**, 1040 (1953).
- [13] D. Bohm, Phys. Rev. **89**, 458 (1953).
- [14] D. Bohm and J.P. Vigier, Phys. Rev. **96**, 208 (1954).
- [15] D. Dürr, S. Goldstein and N. Zanghì, J. Stat. Phys. **67**, 843 (1992); Phys. Lett. A **172**, 6 (1992).
- [16] A. Valentini, Phys. Lett. A **156**, 5 (1991).
- [17] A. Valentini, in: *Chance in Physics: Foundations and Perspectives*, eds. J. Bricmont *et al.* (Springer, Berlin, 2001) (quant-ph/0104067).
- [18] K. Berndl, D. Dürr, S. Goldstein, G. Peruzzi and N. Zanghì, Comm. Math. Phys. **173**, 647 (1995).
- [19] K. Berndl, in: *Bohmian Mechanics and Quantum Theory: an Appraisal*, eds. J.T. Cushing, A. Fine, and S. Goldstein (Kluwer, Dordrecht, 1996).
- [20] W.H. Press, S.A. Teukolsky, W.T. Vetterling and B.P. Flannery, *Numerical Recipes in FORTRAN: the Art of Scientific Computing* (Cambridge University Press, Cambridge, 1992).
- [21] R.H. Parmenter and R.W. Valentine, Phys. Lett. A **201**, 1 (1995).
- [22] R.H. Parmenter and R.W. Valentine, Phys. Lett. A **213**, 319 (1996).
- [23] U. Schwengelbeck and F.H.M. Faisal, Phys. Lett. A **199**, 281 (1995).

- [24] H. Frisk, Phys. Lett. A **227**, 139 (1997).
- [25] C. Dewdney and Z. Malik, Phys. Lett. A **220**, 183 (1996).
- [26] F.H.M. Faisal and U. Schwengelbeck, Phys. Lett. A **207**, 31 (1995).
- [27] G. Iacomelli and M. Pettini, Phys. Lett. A **212**, 29 (1996).
- [28] S. Sengupta and P.K. Chattaraj, Phys. Lett. A **215**, 119 (1996).
- [29] R.H. Parmenter and R.W. Valentine, Phys. Lett. A **227**, 5 (1997).
- [30] H. Westman, unpublished.
- [31] R.C. Tolman, *The Principles of Statistical Mechanics* (Dover, New York, 1979).
- [32] P.C.W. Davies, *The Physics of Time Asymmetry* (University of California Press, Berkeley, 1974).
- [33] C. Dewdney, B. Schwenker and A. Valentini, in preparation.
- [34] L. Sklar, *Physics and Chance: Philosophical Issues in the Foundations of Statistical Mechanics* (Cambridge University Press, Cambridge, 1993).
- [35] *Physical Origins of Time Asymmetry*, eds. J.J. Halliwell, J. Pérez-Mercader, and W.H. Zurek (Cambridge University Press, Cambridge, 1994).
- [36] *Time's Arrows Today: Recent Physical and Philosophical Work on the Direction of Time*, ed. S.F. Savitt (Cambridge University Press, Cambridge, 1995).
- [37] T. Padmanabhan, *Structure Formation in the Universe* (Cambridge University Press, Cambridge, 1993).
- [38] A. Valentini, Phys. Lett. A **158**, 1 (1991).
- [39] A. Valentini, in: *Bohmian Mechanics and Quantum Theory: an Appraisal*, eds. J.T. Cushing, A. Fine, and S. Goldstein (Kluwer, Dordrecht, 1996).
- [40] A. Valentini, Phys. Lett. A **297**, 273 (2002).
- [41] A. Valentini, in: *Non-locality and Modality*, eds. T. Placek and J. Butterfield (Kluwer, Dordrecht, 2002).
- [42] A. Valentini, quant-ph/0309107.
- [43] *The Many-Worlds Interpretation of Quantum Mechanics*, eds. B.S. DeWitt and N. Graham (Princeton University Press, Princeton, 1973).
- [44] D. Deutsch, Proc. Roy. Soc. Lond. A **455**, 3129 (1999).

- [45] D. Wallace, quant-ph/0211104; quant-ph/0303050; quant-ph/0312157.
- [46] H. Barnum, C.M. Caves, J. Finkelstein, C.A. Fuchs and R. Schack, Proc. Roy. Soc. Lond. A **456**, 1175 (2000).
- [47] C.M. Caves, C.A. Fuchs and R. Schack, Phys. Rev. A **65**, 022305 (2002).
- [48] A.M. Gleason, J. Math. Mech. **6**, 885 (1957).
- [49] J.S. Bell, Rev. Mod. Phys. **38**, 447 (1966).
- [50] S. Saunders, Proc. Roy. Soc. Lond. A **460**, 1 (2004).
- [51] W.H. Zurek, Phys. Rev. Lett. **90**, 120404 (2003).
- [52] L. Hardy, quant-ph/0101012; L. Hardy, in: *Non-locality and Modality*, eds. T. Placek and J. Butterfield (Kluwer, Dordrecht, 2002).
- [53] R. Clifton, J. Bub and H. Halvorson, Found. Phys. **33**, 1561 (2003).